Hindawi
Geofluids
Volume 2019, Article ID 4746917, 9 pages
https://doi.org/10.1155/2019/4746917

Research Article

Time-Dependence of Mechanical Property Alterations on Anthracite Coals Treated by Supercritical Carbon Dioxide

Wei Li,[1,2,3] **Bin Pang**,[1,2] **Er-lei Su**,[1,2] **Quanlin Yang**,[4] **Qingquan Liu**,[1,2] **and Yuanping Cheng**[1,2]

[1]*Key Laboratory of Gas and Fire Control for Coal Mines, Ministry of Education, China University of Mining and Technology, Xuzhou 221116, China*
[2]*National Engineering Research Center for Coal Gas Control, China University of Mining and Technology, Xuzhou 221116, China*
[3]*Postdoctoral Workstation, Wanbei Coal Electricity Group Limited Liability Company, Suzhou, 234000 Anhui, China*
[4]*Periodicals Publishing House, Xi'an University of Science and Technology, Xi'an 710054, China*

Correspondence should be addressed to Wei Li; lweisafety@cumt.edu.cn and Yuanping Cheng; ypcheng@cumt.edu.cn

Received 13 June 2019; Accepted 9 August 2019; Published 28 October 2019

Academic Editor: Lionel Esteban

The injection of supercritical carbon dioxide (Sc-CO_2) into coal seams remarkably changes the physical-chemical structures of coal mass and thereby improves coal mechanical properties. In this study, a series of unconfined and triaxial compressive strength tests were performed on anthracite coal samples under the pressure of 8 MPa at the temperature of 35°C for 24 h and 48 h, respectively. Besides, experiments with longer Sc-CO_2 treatment time were carried out on coal mass without stress constraint to observe the damage mode of coal. The results show that Sc-CO_2 treatment obviously alters time-dependent mechanical properties of anthracite coal. The coal samples treated with Sc-CO_2 for 240 h and 960 h show different damage modes from limited fractures to a complicated fracture network. The time-dependence of the mechanical weakening model on Sc-CO_2-treated coal was proposed to explain the link between CO_2 flow and mechanical weakening effect by means of physical-chemical effects on time scales.

1. Introduction

CO_2 sequestration in deep unmineable coal seams, commonly recognized as one of the most promising CO_2 mitigation methods [1–3], can also prominently promote CO_2-enhanced coalbed methane (CO_2-ECBM) recovery [4]. In particular, CO_2 reaches its supercritical state when its pressure and temperature exceed the critical point 7.38 MPa and 31.8°C, respectively. The critical point of CO_2 can be achieved at the depth of around 800 m under normal hydrostatic pressure. Physical properties such as density, diffusivity, and viscosity of supercritical carbon dioxide (Sc-CO_2) change dramatically near the critical point, thus affecting the interaction between rock (coal) and Sc-CO_2 [5, 6]. However, it is necessary to consider certain risks for achieving long-term safe storage of sequestered CO_2.

Unlike subcritical CO_2, Sc-CO_2 exhibits higher adsorption capacity [7] and unique physical properties. According to the extensive present measurements, functional groups and pore structure of each pore phase vary hugely in different coal ranks before and after Sc-CO_2 treatment [8–12]. However, the coal permeability decreases mostly after Sc-CO_2 injection due to the dominant role of sorption-induced swelling [13, 14]. Sc-CO_2 helps to develop seepage-flow pores (mesopores and macropores). In fact, Sc-CO_2 notably alters the development of pores in high-rank and medium-rank coals, whereas it scarcely affects that in low-rank coal. Besides, mineral matters in coal are dissolved and mobilized when they react with Sc-CO_2 [15]. This process of CO_2-ECBM recovery, which alters CO_2-adsorption-induced swelling of coal matrix, influences its hydromechanical properties in turn according to Griffith and Eng [16], and the adsorption effect is able to reduce the strength of materials. The geomechanical properties of CO_2-treated coal are closely related to CO_2 storage volume and stability. A number of

Table 1: Proximate analysis of the coal.

Sample	$R_{o,max}$ (%)	A_{ad} (%)	M_{ad} (%)	V_{ad} (%)
Coal	3.16	22.15	1.55	11.01

$R_{o,max}$ means the maximum vitrinite reflectance, A_{ad} means the ash content (dried basis), M_{ad} means the moisture content (air-dried basis), and V_{ad} means the volatile matter content (air-dried basis).

scholars have explored the influence of CO_2 adsorption on coal strength from subcritical state to supercritical state on both coal powder and tiny cubes. Studies [17, 18] revealed that the strength of low-rank coal decreased greatly with the increase of CO_2 adsorption. In many experiments, considerable reductions in uniaxial compressive strength and Young's modulus were observed as a result of gaseous CO_2 saturation [17, 19, 20]. Sc-CO_2 adsorption can weaken all types of coals [21, 22]. Coal mass gets ductile as the coal becomes plasticized in the process of CO_2 adsorption, and this phenomenon is more notable under the condition of Sc-CO_2 adsorption. It has been put forward that physical and molecule microstructures of coal can be altered by the interaction between CO_2 and coal induced by sorption-induced swelling, pore size reset, hydrocarbon extraction, and macromolecular rearrangement [23–27]. However, the link between the weakening of coal strength and the microcosmic physical-chemical alterations of Sc-CO_2-treated coal is still rarely reported.

Currently, experiments on mechanical comparison before and after Sc-CO_2 did not take time effect into consideration. The time-dependent Sc-CO_2-treated coals provide a good proof for understanding the interaction between Sc-CO_2 and coal, which could also provide insights for coalbed CO_2 storage and Sc-CO_2-treated coal fracturing. Therefore, this study is aimed at investigating the time-dependent mechanical response of anthracite coal samples treated with Sc-CO_2. In addition to uniaxial compression, triaxial compression was applied to coals at different confining pressures to simulate the field stress environment. Then, coal cylinders were treated with Sc-CO_2 for 240 h and 960 h with nonconfining pressure to observe their damage levels. Finally, the time-dependent mechanical weakening effect was explained by introducing the coal cube model and combining the experimental results.

2. Materials and Experiments

2.1. Materials. Experimental coal samples were taken from Daning Coal Mine of Qinshui Basin Coalfield located in the south of Shanxi Province, China. The results of proximate analysis of the coal are presented in Table 1.

In order to conduct uniaxial and triaxial tests, a total of 14 coal samples perpendicular to the bedding were cored from large coal lumps. The samples were 50 mm in diameter and 100 mm in height. It is noteworthy that only homogeneous samples with no visible cleat were used for the mechanical property measurement, so that the effects of anisotropy and heterogeneity on experimental results could be minimized.

2.2. Experimental Procedure. A customized high-pressure reactor that could provide a maximum saturation pressure of 32 MPa was adopted to ensure saturation conditions

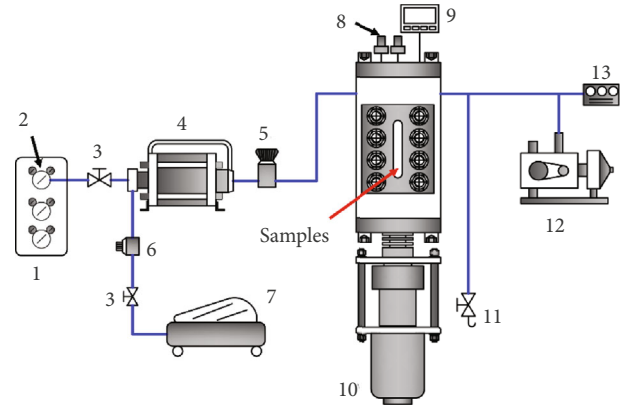

Figure 1: Principle diagram of high-temperature and high-pressure visual reactor. (1) Gas supply; (2) reducing valve; (3) valve; (4) gas booster pump; (5) reducing valve; (6) pressure regulating valve; (7) air compressor; (8) temperature and pressure transducers; (9) temperature and pressure indicator; (10) Sc-CO_2 high-pressure geochemical reactor; (11) safety valve; (12) vacuum pump; (13) vacuum gauge.

(Figure 1). This reactor was equipped with an advanced temperature regulation system that could limit the fluctuation of set temperature to within 0.1°C. In this study, coal samples were saturated in CO_2 at a temperature of 35°C under a pressure of 8 MPa for 12 h or 48 h. Afterwards, the pressure chamber was gradually depressurized at a rate of 0.02 MPa/min, so that physical structure of the coal was unlikely to be damaged as a result of sudden changes in pressure. Then, to avoid the effects of oxidation and humidity, the samples were immediately put into a small sealed bag filled with helium and sent for the mechanical test in the first time.

The mechanical tests were conducted by using an adsorption-permeation-mechanics coupled device whose maximum axial loading and maximum confining loading capacity could reach 600 KN. Axial and radial strain sensors, with maximum test ranges of 8 mm and 4 mm, respectively, were equipped for the sample deformation tests during stress loading, as exhibited in Figure 2. In this study, two main test scenarios were applied. First, the uniaxial and triaxial experiments were performed on raw coal samples under confining pressures of 0, 2, 4, and 6 MPa and under an axial loading rate of 0.3 MPa/min until the samples failed. During the experiments, the peak strength, axial strain, and radial strain were observed and recorded. Second, under the same confining pressure conditions, the procedures of uniaxial and triaxial tests were repeated on Sc-CO_2-treated samples for 12 h and 48 h.

3. Results

3.1. Strength Evolution of Time-Dependent Sc-CO_2 Treatment on Coal. After the uniaxial and triaxial experiments, the deviatoric stress- (σ_1-σ_3) strain behaviors for the raw and Sc-CO_2-treated samples under different confining pressures were obtained, as illustrated in Figure 3. The axial strain (ε_1), radial strain (ε_2), and volumetric strain (ε_v)

Figure 2: Triaxial mechanical device for raw and Sc-CO_2-treated coal samples.

vary inconsistently with the deviatoric stress. In fact, three stages, namely, volume compression, constant volume, and volume dilatation, can be observed in the deviatoric stress-strain curves. As can be found in Figure 3, despite the small values of slopes of axial and radial strain curves, the axial and radial strains rise rapidly as the confining pressure (σ_3) goes up. In this process, brittle strain is gradually turned into plastic deformation, and higher confining pressure corresponds to higher peak strength.

Compared with the raw coal samples, the samples treated with Sc-CO_2 for 12 h and 48 h have smaller values of peak strength and strain under the same confining pressure, and the values decreased significantly. Under uniaxial compression, strengths of the samples saturated for 12 h are reduced by up to 4.49 MPa, corresponding to an unconfined compressive strength reduction of 25.6% under initial conditions, and the reduction reaches 45.15% after Sc-CO_2 treatment for 48 h.

As can be observed in Figure 4, higher confining pressure corresponds to higher compressive strength when a coal sample fails, and the compressive strength decreases with the Sc-CO_2 treatment time under the same confining pressure. Under 4 MPa confining pressure, the compressive strength of raw coal is 47.8 MPa, a decrease of 29.16% and 47.09% compared with those of samples treated with Sc-CO_2 for 12 h and 48 h, respectively. The compressive strength exhibits the same variation tendency under 2 MPa and 6 MPa confining pressures. The Mohr-Coulomb strength criterion could be used to determine the failure of coal samples under constant confining pressure, as shown below.

$$\sigma_1 = \frac{1+\sin\varphi}{1-\sin\varphi}\sigma_3 + 2C\frac{\cos\varphi}{1-\sin\varphi}, \quad (1)$$

where C is the cohesion and φ is the internal friction angle. The cohesion and internal friction angle could be obtained in light of the criterion, as shown in Table 2.

Both cohesion and internal friction angle of coal samples undergo a decrease after Sc-CO_2 treatment. The cohesions of samples decrease by 8.9% and 27.4% after Sc-CO_2 treatment for 12 h and 48 h, respectively. The internal friction angles of samples drop by 8.36° and 13.71°, respectively, accounting for 17.53% and 28.75% of that of raw coal. Cohesion is the mutual attraction formed by molecular forces in the adjacent parts of coal, and frictional force and chain effect of coal matrix are expressed by internal frictional angle. A larger internal frictional angle implies higher mechanical strength. The Sc-CO_2 treatment obviously weakens the strength of coal samples, and the weakening effect is more obvious with a longer Sc-CO_2 treatment time.

3.2. Strain Evolution of Time-Dependent Sc-CO_2 Treatment on Coal. Coal deformation, which is reflected by Young's modulus and Poisson's ratio, could be calculated according to the deviatoric stress and strain obtained in the uniaxial and triaxial experiments (Table 3). The experimental results reveal that during SC-CO_2 treatment, SC-CO_2 saturation influences Young's modulus and Poisson's ratio in addition to the strength of anthracite coal. Young's moduli drop by 25% and 40%, while Poisson's ratios jump by 19.23% and 30.76% on average after Sc-CO_2 treatment for 12 h and 48 h (8 MPa), respectively. As the confining pressure increases from 0 to 6 MPa, the Young's modulus grows from 2716 MPa to 3422 MPa during the test of 12 h Sc-CO_2 treatment. Meanwhile, Poisson's ratio shows the same tendency, that is, it increases by a factor of 1.09-1.125 for the raw and treated coal samples. It can be concluded that the confining pressure and the Sc-CO_2 treatment share a competitive relationship in terms of Young's modulus.

Coal is a highly brittle material that rarely moves due to its high-energy structure in a glassy state. The CO_2 adsorbed into coal matrix can improve its polymer structure and thus expand the free volume. As a result, the ductile properties of coal mass get promoted, which reduces Young's modulus and raises Poisson's ratio [28, 29].

3.3. Pore and Fracture Distribution of Sc-CO_2-Treated Coal. The cumulative pore volume curves of raw and Sc-CO_2-treated coal samples were analyzed by means of mercury intrusion porosimetry (MIP), as displayed in Figure 5(a). The pore characteristics of coal samples can be explored according to the widths of hysteresis loops and the volumetric difference between mercury injection and extrusion curves. As can be seen from Figure 5, the cumulative mercury intrusion volume rises slowly when the pressure is lower than 20 MPa, while it increases sharply after the pressure exceeds 20 MPa. Compared with the raw coal samples, the mercury intrusion curves of Sc-CO_2-treated coal samples increase slower, indicating that Sc-CO_2-treated coal samples boast more uniform pore size distribution. Moreover, the cumulative mercury intrusion (0.302 cm^3/g) of Sc-CO_2-treated coal samples is 10.22% higher than that (0.274 cm^3/g) of raw coal samples. The pore size in the Sc-CO_2-treated samples alters, and the total pore volume expands. Besides, the hysteresis loop of Sc-CO_2-treated samples increases from 0.0028 cm^3/g to 0.0043 cm^3/g, which may result from

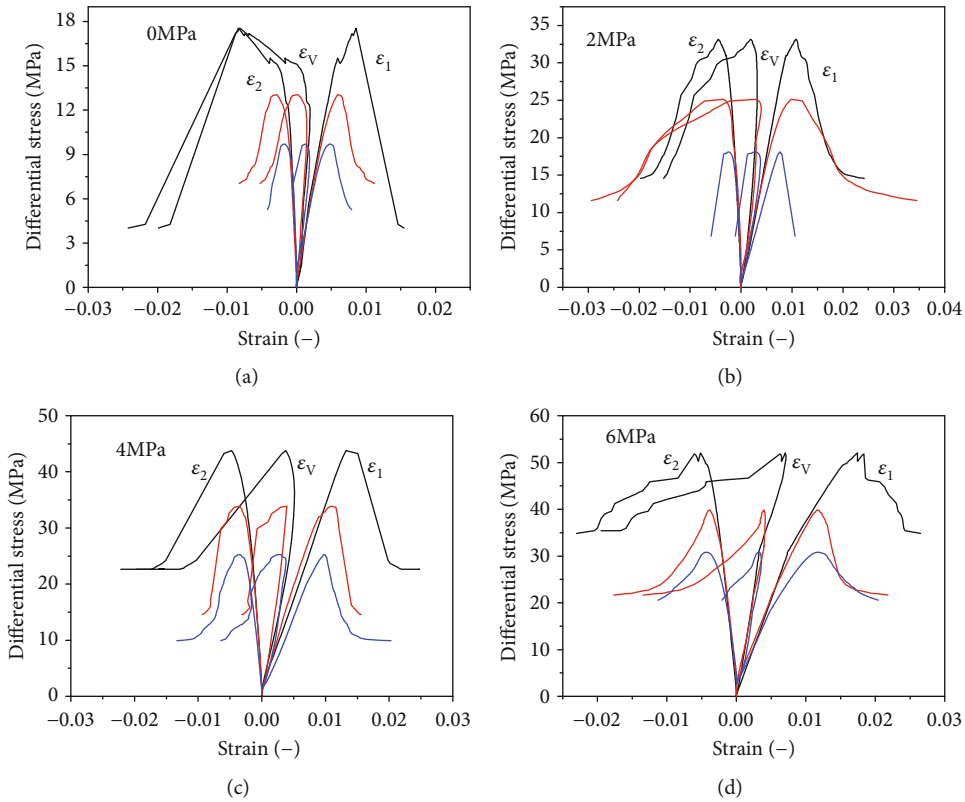

Figure 3: Deviatoric stress-strain relation curve of raw and Sc-CO_2-treated coal samples (black line = raw sample, red line = 12 h treated, and blue line = 48 h treated) under different confining pressures ((a) confining pressure 0 MPa, (b) confining pressure 2 MPa, (c) confining pressure 4 MPa, (d) confining pressure 6 MPa).

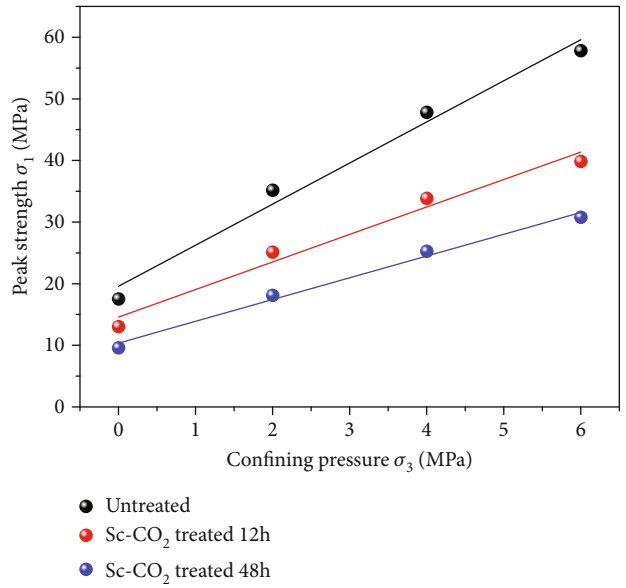

Figure 4: Relationship between maximum and minimum principal stresses of coal under the same treatment conditions.

the decrease in semiclosed pores, the formation of more open pores, and the development of pore network. This is probably because Sc-CO_2 dissolves and mobilizes hydrocarbons, leading to adsorption-induced deformation and physical constriction [31, 32].

Table 2: Cohesion and internal friction angle of coal samples under different conditions.

Coal samples	Cohesion (MPa)	Internal friction angle (°)
Raw coal samples	3.79	47.69
Samples treated with Sc-CO_2 for 12 h	3.45	39.33
Samples treated with Sc-CO_2 for 48 h	2.75	33.98

Pore size distribution can be seen more intuitively from Figure 5(b). The mercury intrusion volume of mesopores and macropores in coal samples increases significantly by 0.0037 cm^3/g after Sc-CO_2 treatment, while that of transition pores and micropores decreases slightly by 0.0009 cm^3/g. Firstly, the CO_2 molecules were injected into the coal seam flow through the mesopores and macropores in the form of laminar flow or turbulent flow. The channel of gas flow expands when the volume of mesopores and macropores increases. Previous studies [29] also revealed that Sc-CO_2 treatment could result in smoother pore surface of coal samples and better connectivity of pores, which conduces to the diffusion and seepage of gas molecules. Eventually, after the Sc-CO_2 treatment, mesopores and macropores develop faster and better in coal, which may help gas to desorb and diffuse from coal matrix and transport in coal fracture.

Table 3: Experimental results of Young's modulus and Poisson's ratio obtained from each test.

Coal samples	Confining pressure (MPa)	Young's modulus (MPa)		Poisson's ratio (%)	
		Measured	Average	Measured	Average
Raw coal samples	0	3668	4054	0.24	0.26
	2	3959		0.26	
	4	4225		0.25	
	6	4364		0.27	
Samples treated with Sc-CO_2 for 12 h	0	2716	3040	0.30	0.31
	2	2920		0.29	
	4	3102		0.32	
	6	3422		0.33	
Samples treated with Sc-CO_2 for 48 h	0	2136	2432	0.33	0.34
	2	2372		0.32	
	4	2582		0.35	
	6	2638		0.36	

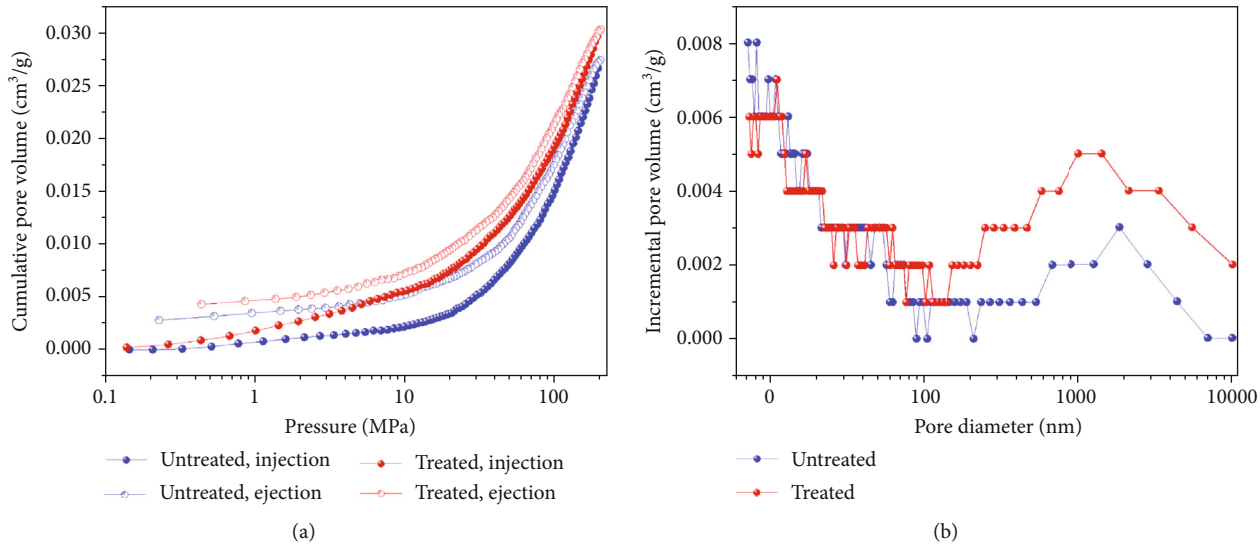

Figure 5: Pore volume (a) and Pore size distribution (b) of raw and Sc-CO_2-treated coal samples by means of MIP [30].

3.4. Time-Dependent Sc-CO_2 Treatment on Coal Damage. Two sets of coal cylinders were treated with Sc-CO_2 (9.65 MPa, 35°C) without stress constraint for 240 h and 960 h, respectively. Sc-CO_2 was released at the rate of 0.015 MPa/min to prevent the rapid decrease in gas pressure. Figure 6 displays the damage modes of Sc-CO_2-treated samples in different time periods.

The coal samples saturated with Sc-CO_2 for 240 h present limited fractures and cracks compared with raw coal samples. However, after Sc-CO_2 treatment for 960 h, the coal samples, which have a more complicated fracture network, lose the main mechanical strength and become looser with poor cohesion. In fact, it can be easily stripped by hand. Judging by the crack shapes, the failure belongs to tensile failure due to compression that may be caused by coal matrix swelling. This is consistent with Zhang et al.'s observation [33]. From the appearance, there are some assumptions that the coal damage is attributed to the time-dependent Sc-CO_2 transport and adsorption-induced swelling, and it has been recently observed that the unswelling phase is due to the induced swelling stresses [34]. These stress fields are highly anisotropic; the maximum effective stresses concentrate on the mineral surface in most cases; the Von Mises stresses continuously rise with the increase of coal matrix swelling until the coal fails [33]. CO_2 saturation alters the unconfined compressive stress failure modes of the shear-dominant failure mechanism in the raw coal into the failure along the cleat, the tensile failure plane, and the splitting failure plane system [22, 29, 35]. This is mainly because of the generation of secondary cracks resulted from CO_2 adsorption-induced heterogeneous swelling and local swelling stress.

4. Discussion

4.1. Time-Dependence of Mechanical Weakening Effect on Sc-CO_2 Treatment. The coal cube model, which is widely used to

(a) (b)

Figure 6: Damage appearance of Sc-CO_2-treated coal samples under different saturated times: (a) and (b) are a comparison before and after treatments for 240 h and 960 h, respectively.

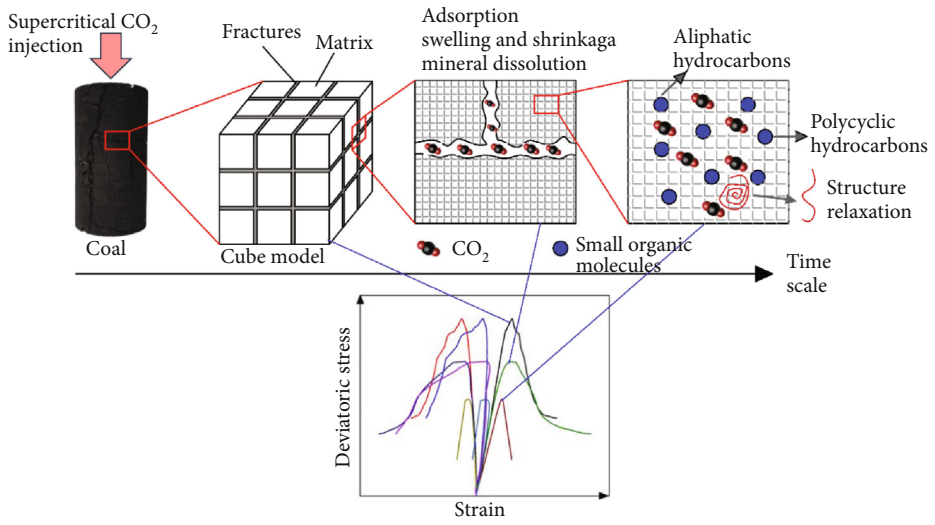

Figure 7: Time-dependence of mechanical weakening on Sc-CO_2 treatment with coal cube model.

describe gas transport and permeability evolution from coal matrix to fractures [36, 37], also matches well with Sc-CO_2 injection and coal strength evolution with time. Hence, the model is introduced to reveal the time-dependence of coal mechanical property variation after Sc-CO_2 injection (Figure 7). The two parts of fracture and matrix strength weakening effects are attributed to stress-strain evolution with time.

Based on the above observations, the Sc-CO_2 treatment not only causes a decrease in the mechanical properties (peak strength, elastic modulus, cohesion, and internal frictional angle) of coal in triaxial or uniaxial stress environments but also modifies the properties of coal mass, leading to a transition from brittle failure to ductile failure. The coal treated with Sc-CO_2 for 48 h undergoes a more obvious decrease in mechanical properties than the coal treated for 12 h. Other experiments suggest that the mechanical properties of Sc-CO_2-treated coal will not decrease continuously over time and can be presented using a simple Langmuir type equation [38]. Flow of Sc-CO_2 through the cleats is driven by pressure and can be described using Darcy's law at first. The adsorption-induced swelling and the reduction in fracture surface energy opens the fractures, hence reducing tensile strength and facilitating crack formation. As the Sc-CO_2 treatment leads to the dissolution of minerals, fractures become smoother and apertures expand. When the stress of adsorption-induced swelling exceeds the matrix cohesion, a new crack surface is formed [16]. Sc-CO_2 can enhance the

coal permeability by promoting the development of micropores, mesopores, and macropores in coal. In this way, fracture morphology is transformed through mineral dissolution, desorption shrinkage, and new minor crack generation, which all contributes to raising the coal porosity and lowering the coal strength.

However, the flow through the coal matrix, which is modeled by Fick's law of diffusion, is assumed to be driven by the concentration difference and needs a long time to reach full Sc-CO_2 saturation. The coal strength further declines as the Sc-CO_2 diffuses into coal matrix after long-term treatment. A covalently cross-linked, three-dimensional macromolecular model, together with an intra- and intermolecular model [39, 40], has been widely recognized to describe the organic matrix. Former research of the authors suggested that the injection of Sc-CO_2 into coal can lead to the swelling effect, namely, the viscoelastic relaxation of its highly cross-linked macromolecular structure. Sc-CO_2 is capable of mobilizing small hydrocarbon molecules from the coal matrix [41] (Figure 7). That is, Sc-CO_2 can reduce the intermolecular force in coal atoms. From a macro perspective, the effect is manifested by the decreases in cohesion and internal friction angle with the decrease in coal strength and deformation. The time-dependent model of coal mechanical property weakening contributes to the time-dependent Sc-CO_2 transport through coal mass fracture and matrix and physical-chemical reactions in the corresponding position.

4.2. Implication for In Situ Sc-CO_2 Coalbed Injection and Storage. The preferable coal seams for CO_2 sequestration exist at depths of greater than 800 m. The interaction between coal and Sc-CO_2 and the mechanical strength evolution have been widely studied in recent years [22, 29, 38]. The time-dependent triaxial experiments (up to 6 MPa) indicate that the longer the treatment time is, the more significantly the peak strength decreases. The failure mode of coal transits from brittle failure to ductile failure with the rise of confining pressure. In addition, the stress magnitude is much higher than the value obtained in in situ experiments at depths of over 800 m, implying that the further decrease in coal permeability is dominantly controlled by the swelling induced by Sc-CO_2 sorption [42]. The ductile deformation of Sc-CO_2-treated coal causes the fractures to close and the CO_2 to desorb under high effective stress, which also lowers coal permeability to hinder further transport of CO_2. It is also found that the CO_2 injection volume drops in a short period of time due to the sorption-induced swelling as well as high stress in the field [43, 44]. According to above findings, the coal seam might not be a suitable layer for long-term CO_2 storage despite its great adsorption affinity. Nowadays, Sc-CO_2 fracturing is applied to enhancing CBM/shale or increasing permeability to improve gas recovery [45]. The injected Sc-CO_2 should crack the coal seam as quickly as possible to prevent plastic deformation of fully saturated coal. The fractures generated during hydrofracturing heal with the release of pressure because of the plastic deformation nature of CO_2-saturated coal, creating unfavorable formation properties. These observations imply that the ductile behavior of Sc-CO_2-adsorbed coal is significantly enhanced with the plasticization of coal, and the surface energy reduces critically at the beginning of CO_2 sequestration. However, the effect of Sc-CO_2 is reduced over time. This laboratory tests provide a better vision for the effects of CO_2 sequestration or ECBM in coal seams in a controlled environment.

5. Conclusion

Sc-CO_2 treatment significantly alters time-dependent mechanical properties of anthracite coal. Greater decreases in peak strength were observed after Sc-CO_2 treatment for 12 h and 48 h. Higher confining pressure corresponds to greater compressive strength when the coal samples fail. Besides, the strain of coal experiences a transition from brittle to ductile as the confining pressure rises and Sc-CO_2 treatment time prolongs. As the treatment time passes, Sc-CO_2 saturation reduces cohesion, internal friction angle, and Young's modulus and raises Poisson's ratio, which also controls the evolution of coal strain and failure. Sc-CO_2 treatment facilitates the development of mesopores and macropores in coal by dissolving and mobilizing hydrocarbons. The coal samples treated with Sc-CO_2 for 240 h and 960 h show a different damage appearance, as it alters from limited fractures to a complicated fracture network. A time-dependent Sc-CO_2 flow through the coal matrix and the physical-chemical reaction model was proposed to build the link between coal fracture and matrix mechanical weakening effect from experiments. Sc-CO_2 interacts with coal in a complicated way after CO_2 flows and diffuses from particle coal to massive coal through fractures and coal matrix. Moreover, the saturation of CO_2 can lead to the swelling, dissolution, and surface energy reduction of coal with the passage of time, which in turn has a large influence on coal strength and fracture development. The time-dependence of Sc-CO_2 transport and interaction with coal may have profound meanings for coalbed CO_2 storage and Sc-CO_2 organic rock fracturing.

Data Availability

The data used to support the findings of this study are available from the corresponding author upon request.

Conflicts of Interest

The authors declare that they have no conflicts of interest.

Acknowledgments

This research was financially supported by the National Natural Science Foundation of China (No. 51874295), the Fundamental Research Funds for the Central Universities (grant No. 2015XKMS006), and a project funded by the priority academic development program of Jiangsu Higher Education Institutions. The authors would like to thank the China Scholarship Council for the financial support.

References

[1] S. Bachu, "Carbon dioxide storage capacity in uneconomic coal beds in Alberta, Canada: methodology, potential and site identification," *International Journal of Greenhouse Gas Control*, vol. 1, no. 3, pp. 374–385, 2007.

[2] A. S. Ranathunga, M. S. A. Perera, and P. G. Ranjith, "Deep coal seams as a greener energy source: a review," *Journal of Geophysics and Engineering*, vol. 11, no. 6, article 063001, 2014.

[3] C. M. White, D. H. Smith, K. L. Jones et al., "Sequestration of carbon dioxide in coal with enhanced coalbed methane recovery - a review," *Energy & Fuels*, vol. 19, no. 3, pp. 659–724, 2005.

[4] M. Mazzotti, R. Pini, and G. Storti, "Enhanced coalbed methane recovery," *The Journal of Supercritical Fluids*, vol. 47, no. 3, pp. 619–627, 2009.

[5] W. Li, Y. P. Cheng, L. Wang, H. X. Zhou, H. F. Wang, and L. G. Wang, "Evaluating the security of geological coalbed sequestration of supercritical CO_2 reservoirs: the Haishiwan coalfield, China as a natural analogue," *International Journal of Greenhouse Gas Control*, vol. 13, pp. 102–111, 2013.

[6] E. Liteanu, C. J. Spiers, and J. H. P. de Bresser, "The influence of water and supercritical CO_2 on the failure behavior of chalk," *Tectonophysics*, vol. 599, pp. 157–169, 2013.

[7] S. Day, R. Fry, R. Sakurovs, and S. Weir, "Swelling of coals by supercritical gases and its relationship to sorption," *Energy & Fuels*, vol. 24, no. 4, pp. 2777–2783, 2010.

[8] B. B. Gathitu, W.-Y. Chen, and M. McClure, "Effects of coal interaction with supercritical CO_2: physical structure," *Industrial & Engineering Chemistry Research*, vol. 48, no. 10, pp. 5024–5034, 2009.

[9] J. W. Larsen, "The effects of dissolved CO_2 on coal structure and properties," *International Journal of Coal Geology*, vol. 57, no. 1, pp. 63–70, 2004.

[10] M. Mastalerz, A. Goodman, and D. Chirdon, "Coal lithotypes before, during, and after exposure to CO_2: insights from direct Fourier transform infrared investigation," *Energy & Fuels*, vol. 26, no. 6, pp. 3586–3591, 2012.

[11] D. Zhang, L. Gu, S. Li, P. Lian, and J. Tao, "Interactions of supercritical CO_2 with coal," *Energy & Fuels*, vol. 27, no. 1, pp. 387–393, 2013.

[12] K. Zhang, Y. Cheng, K. Jin et al., "Effects of supercritical CO_2 fluids on pore morphology of coal: implications for CO_2 geological sequestration," *Energy & Fuels*, vol. 31, no. 5, pp. 4731–4741, 2017.

[13] A. S. Ranathunga, M. S. A. Perera, P. G. Ranjith, X. G. Zhang, and B. Wu, "Super-critical carbon dioxide flow behaviour in low rank coal: a meso-scale experimental study," *Journal of CO2 Utilization*, vol. 20, pp. 1–13, 2017.

[14] V. Vishal, "In-situ disposal of CO_2: liquid and supercritical CO_2 permeability in coal at multiple down-hole stress conditions," *Journal of CO2 Utilization*, vol. 17, pp. 235–242, 2017.

[15] P. Massarotto, S. D. Golding, J. S. Bae, R. Iyer, and V. Rudolph, "Changes in reservoir properties from injection of supercritical CO_2 into coal seams — a laboratory study," *International Journal of Coal Geology*, vol. 82, no. 3-4, pp. 269–279, 2010.

[16] A. A. Griffith, "VI. The phenomena of rupture and flow in solids," *Philosophical Transactions of the Royal Society A*, vol. 221, pp. 163–198, 1921.

[17] N. I. Aziz and W. Ming-Li, "The effect of sorbed gas on the strength of coal – an experimental study," *Geotechnical & Geological Engineering*, vol. 17, no. 3/4, pp. 387–402, 1999.

[18] A. Czapliński and S. Hołda, "Changes in mechanical properties of coal due to sorption of carbon dioxide vapour," *Fuel*, vol. 61, no. 12, pp. 1281-1282, 1982.

[19] K. H. S. M. Sampath, M. S. A. Perera, P. G. Ranjith, and S. K. Matthai, "CO_2 interaction induced mechanical characteristics alterations in coal: a review," *International Journal of Coal Geology*, vol. 204, pp. 113–129, 2019.

[20] D. R. Viete and P. G. Ranjith, "The effect of CO_2 on the geomechanical and permeability behaviour of brown coal: implications for coal seam CO_2 sequestration," *International Journal of Coal Geology*, vol. 66, no. 3, pp. 204–216, 2006.

[21] M. S. A. Perera, A. S. Ranathunga, and P. G. Ranjith, "Effect of coal rank on various fluid saturations creating mechanical property alterations using Australian coals," *Energies*, vol. 9, no. 6, p. 440, 2016.

[22] M. S. A. Perera, P. G. Ranjith, and D. R. Viete, "Effects of gaseous and super-critical carbon dioxide saturation on the mechanical properties of bituminous coal from the southern Sydney Basin," *Applied Energy*, vol. 110, pp. 73–81, 2013.

[23] S. Day, R. Fry, and R. Sakurovs, "Swelling of Australian coals in supercritical CO_2," *International Journal of Coal Geology*, vol. 74, no. 1, pp. 41–52, 2008.

[24] Z. Majewska, S. Majewski, and J. Ziętek, "Swelling and acoustic emission behaviour of unconfined and confined coal during sorption of CO_2," *International Journal of Coal Geology*, vol. 116-117, pp. 17–25, 2013.

[25] M. Mirzaeian, P. J. Hall, and H. F. Jirandehi, "Study of structural change in Wyodak coal in high-pressure CO_2 by small angle neutron scattering," *Journal of Materials Science*, vol. 45, no. 19, pp. 5271–5281, 2010.

[26] L. Wang, Y. Cheng, and W. Li, "Migration of metamorphic CO_2 into a coal seam: a natural analog study to assess the long-term fate of CO_2 in Coal Bed Carbon Capture, Utilization, and Storage Projects," *Geofluids*, vol. 14, no. 4, 390 pages, 2014.

[27] K. Zhang, Y. Cheng, W. Li, D. Wu, and Z. Liu, "Influence of supercritical CO_2 on pore structure and functional groups of coal: implications for CO_2 sequestration," *Journal of Natural Gas Science and Engineering*, vol. 40, pp. 288–298, 2017.

[28] C. Ö. Karacan, "Heterogeneous sorption and swelling in a confined and stressed coal during CO_2 injection," *Energy & Fuels*, vol. 17, no. 6, pp. 1595–1608, 2003.

[29] A. S. Ranathunga, M. S. A. Perera, P. G. Ranjith, and H. Bui, "Super-critical CO_2 saturation-induced mechanical property alterations in low rank coal: an experimental study," *The Journal of Supercritical Fluids*, vol. 109, pp. 134–140, 2016.

[30] W. Li, Z. Liu, E. Su, and Y. Cheng, "Experimental investigation on the effects of supercritical carbon dioxide on coal permeability: implication for CO_2 injection method," *Energy & Fuels*, vol. 33, no. 1, pp. 503–512, 2019.

[31] J.-S. Bae, S. K. Bhatia, V. Rudolph, and P. Massarotto, "Pore accessibility of methane and carbon dioxide in coals," *Energy & Fuels*, vol. 23, no. 6, pp. 3319–3327, 2009.

[32] J. J. Kolak and R. C. Burruss, "Geochemical investigation of the potential for mobilizing non-methane hydrocarbons during carbon dioxide storage in deep coal beds," *Energy & Fuels*, vol. 20, no. 2, pp. 566–574, 2006.

[33] Y. Zhang, M. Lebedev, M. Sarmadivaleh, A. Barifcani, and S. Iglauer, "Swelling-induced changes in coal microstructure

due to supercritical CO_2 injection," *Geophysical Research Letters*, vol. 43, no. 17, pp. 9077–9083, 2016.

[34] Y. Zhang, M. Lebedev, M. Sarmadivaleh, A. Barifcani, and S. Iglauer, "Change in geomechanical properties of limestone due to supercritical CO_2 injection," in *SPE Asia Pacific Oil & Gas Conference and Exhibition*, pp. 25–27, Perth, Australia, 2016.

[35] H. Yin, J. Zhou, X. Xian et al., "Experimental study of the effects of sub- and super-critical CO_2 saturation on the mechanical characteristics of organic-rich shales," *Energy*, vol. 132, pp. 84–95, 2017.

[36] L. D. Connell, M. Lu, and Z. Pan, "An analytical coal permeability model for tri-axial strain and stress conditions," *International Journal of Coal Geology*, vol. 84, no. 2, pp. 103–114, 2010.

[37] J. E. Warren and P. J. Root, "The behavior of naturally fractured reservoirs," *Society of Petroleum Engineers Journal*, vol. 3, no. 3, pp. 245–255, 1963.

[38] A. S. Ranathunga, M. S. A. Perera, and P. G. Ranjith, "Influence of CO_2 adsorption on the strength and elastic modulus of low rank Australian coal under confining pressure," *International Journal of Coal Geology*, vol. 167, pp. 148–156, 2016.

[39] M. Nishioka, "The associated molecular nature of bituminous coal," *Fuel*, vol. 71, no. 8, pp. 941–948, 1992.

[40] V. Romanov, "Coal chemistry for mechanical engineers: from macromolecular thermodynamics to reservoir simulation," *Energy & Fuels*, vol. 21, no. 3, pp. 1646–1654, 2007.

[41] W. Li, J.-t. Zhu, Y.-p. Cheng, and S.-q. Lu, "Evaluation of coal swelling-controlled CO_2diffusion processes," *Greenhouse Gases: Science and Technology*, vol. 4, no. 1, pp. 131–139, 2014.

[42] V. Vishal and T. N. Singh, "A laboratory investigation of permeability of coal to supercritical CO_2," *Geotechnical and Geological Engineering*, vol. 33, no. 4, pp. 1009–1016, 2015.

[43] X. Cui, R. M. Bustin, and L. Chikatamarla, "Adsorption-induced coal swelling and stress: implications for methane production and acid gas sequestration into coal seams," *Journal of Geophysical Research*, vol. 112, no. B10, 2007.

[44] M. Fujioka, S. Yamaguchi, and M. Nako, "CO_2-ECBM field tests in the Ishikari Coal Basin of Japan," *International Journal of Coal Geology*, vol. 82, no. 3-4, pp. 287–298, 2010.

[45] R. S. Middleton, J. W. Carey, R. P. Currier et al., "Shale gas and non-aqueous fracturing fluids: opportunities and challenges for supercritical CO_2," *Applied Energy*, vol. 147, pp. 500–509, 2015.